Early brain-wide disruption of sleep microarchitecture in Amyotrophic Lateral Sclerosis.

Christina Lang[1,2†], Simon J. Guillot[3†], Dorothee Lule[1,2], Luisa T. Balz[1,2], Antje Knehr[1,2], Patrick Weydt1[,4], Johannes Dorst[1,2], Katharina Kandler[1,2], Hans-Peter Muller[1,2], Jan Kassubek[1,2], Laura Wassermann[1], Sandrine Da Cruz[5], Francesco Roselli[,2], Albert C. Ludolph[1,2*], Matei Bolborea[3*], Luc Dupuis[3*]

Affiliations.

[1]Department of Neurology, University Hospital of Ulm; Ulm, Germany

[2]Deutsches Zentrum für Neurodegenerative Erkrankungen (DZNE); Ulm, Germany

[3]University of Strasbourg, INSERM, Strasbourg Translational Neuroscience & Psychiatry STEP – CRBS, UMR-S 1329; Strasbourg, France

[4]Deutsches Zentrum für Neurodegenerative Erkrankungen (DZNE); Bonn, Germany

[5] VIB-KU Leuven Center for Brain and Disease Research and Department of Neurosciences, KU Leuven, Leuven, Belgium

*Co-senior and corresponding authors. Email: albert.ludolph@uni-ulm.de; mbolborea@unistra.fr; ldupuis@unistra.fr;

† CL and SJG contributed equally to this investigation.

Conflict-of-interest statement

The authors have declared that no conflict of interest exists.

Abstract

Background: Amyotrophic lateral sclerosis (ALS), the major adult-onset motor neuron disease, is preceded by an early period unrelated to motor symptoms, including altered sleep, with increased wakefulness and decreased deep NREM. Whether these alterations in sleep macroarchitecture are associated with, or even precede abnormalities in sleep-related EEG features remains unknown.

Methods: Here, we characterised sleep microarchitecture using polysomnography in patients with ALS (n=33) and controls (n=32), and in asymptomatic carriers of *SOD1* or *C9ORF72* mutations (n=57) and non-carrier controls (n=30). Patients and controls with factors that could confound sleep structure, including respiratory insufficiency, were prospectively excluded. Results were complemented in three ALS mouse models (*Sod1*^{G86R}, *Fus*$^{\Delta NLS/+}$ and *TDP-43*^{Q331K}).

Results: We observed a brain-wide reduction in the density of sleep spindles, slow oscillations and K-complexes in both early-stage ALS patients and presymptomatic gene carriers. These defects in sleep spindles and slow oscillations correlate with cognitive performance in both cohorts, particularly with scores on memory, verbal fluency and language function. Alterations in sleep microarchitecture were replicated in three mouse models and decreases in sleep spindles were rescued following intracerebroventricular supplementation of MCH or by the oral administration of a dual orexin receptor antagonist.

Conclusion: Sleep microarchitecture is associated with cognitive deficits and is causally linked to aberrant MCH and orexin signalling in ALS.

Funding: This work was funded by Agence Nationale de la Recherche (ANR-24-CE37-4064, ANR-10-IDEX-0002, ANR-20-SFRI-0012), Fondation Thierry Latran, Association Francaise de Recherche sur la sclérose latérale amyotrophique, Association Française contre les Myopathies (#28944), TargetALS and JPND.

Introduction.

Amyotrophic lateral sclerosis (ALS) is a fatal and rapidly progressive disease affecting upper and lower motor neurons in adults, with a median survival of three to four years after the onset of motor symptoms. ALS usually manifests between 60 and 70 years of age (1, 2), and most cases lack a family history. However, 5-10% of ALS cases are familial cases, with more than 40 distinct genes currently associated, and mutations in *C9ORF72, SOD1*, *TARDBP,* and *FUS* being recognised as major genetic causes of ALS (1, 2).

It is generally considered that ALS patients do not exhibit clinical manifestations before the onset of motor symptoms. Circulating neurofilament levels, a reliable biomarker of (motor) axonal injury, increase at the time of motor symptoms onset but not one to two years prior to it (3, 4). Clinically, most presymptomatic gene carriers do not show even mild motor impairment within this timeframe (4, 5). However, a number of early non-motor signs, such as weight loss (6-10) or cognitive impairment (11, 12), are known to be present in the prodromal phase, many years before the appearance of motor symptoms.

In recent research, we identified sleep alterations as a novel early non-motor sign of ALS. We investigated sleep in two cohorts of ALS patients devoid of respiratory insufficiency and in presymptomatic gene carriers. In both cohorts, we observed significant defects in sleep macroarchitecture characterised by increased wake and reduced deep sleep (NREM2/3) (13). These defects were detectable at least 10-15 years before the expected onset of motor symptoms in presymptomatic gene carriers and correlated with cognitive scores (13). Similar macroarchitectural alterations were observed in mouse models of familial ALS (13).

While previous studies established sleep defects as an early phenotype in future ALS patients, we wish now to explore how sleep-related electroencephalogram (EEG) hallmarks were

affected in ALS that could be used in regular clinical assessment. The different sleep stages are distinguished by specific graphoelements in the EEG that reflect the activation of particular cortical and subcortical pathways. These neuronal activity patterns are considered manifestations of the microarchitecture of sleep. Key EEG hallmarks include sleep spindles, bursts of 11–15 Hertz activity (Hz, sigma frequency band), typically between 0.5 and 2 seconds (s) in duration (14, 15), as well as slow oscillations (<1.5 Hz) and K-complexes (<1Hz), which are all involved in NREM sleep continuity and the role of sleep in memory consolidation and cognitive function (14, 16). A disruption in the microarchitecture of sleep could be caused by specific changes in neuroanatomical pathways and thus also serve as a potential biomarker for neuronal changes or pathological conversion. Here, we analysed sleep microarchitecture components in ALS patients, presymptomatic gene carriers and mouse models (13). We observed a widespread reduction in sleep spindles, slow oscillations and K-complexes that correlated with cognitive function. We also observed similar changes in mouse models and demonstrated that they can be corrected by MCH supplementation or the administration of a dual orexin receptor antagonist. Thus, sleep microarchitecture dynamics are affected early in ALS and linked to hypothalamic dysfunction.

Results

Early ALS patients exhibit brain-wide decreased sleep spindle density

To examine the extent of alterations in sleep microarchitecture in individuals with early-stage amyotrophic lateral sclerosis (ALS), we took advantage of polysomnography acquired in a previous cohort study (13). Characteristics of included patients are described in Figure 1A and detailed in Table 1. We prospectively excluded patients and controls with abnormal capnographies, ensuring that the observed sleep defects were not secondary to respiratory insufficiency. Given the high prevalence of periodic limb movements in neurological diseases and an increased rate of individuals with sleep-disordered breathing among ALS patients, we determined the following exclusion criteria: Apnea-Hypopnea Index (AHI) of >20 and Periodic Limb Movement Index (PLMI) of >50, reasoning that individuals above these thresholds would very likely display altered sleep architecture unrelated to ALS. We also did not observe REM behaviour disorder or REM sleep without atonia in patients or subjects included using established criteria (17). Furthermore, other potential factors contributing to alterations in sleep architecture, including sleep-related breathing disorders and periodic limb movements during sleep, were considered exclusion criteria. No significant differences were observed between the ALS patients and the control group with regard to age, sex or body mass index. Two ALS patients (6%) were taking sleep-inducing medication (one melatonin 2 mg, one mirtazapine 22.5 mg), while no participants in the healthy control group or the presymptomatic gene carrier cohort were taking such medication.

Consistent with the previously observed strong defect in NREM2 and -3, we observed a pronounced decrease in sleep spindle density and their root mean square in ALS patients (Figure 2A-B), while their amplitude was unchanged (Figure 2B). Topographically, we observed a significant decrease in sleep spindle density in both frontal and central electrodes (Figure 2C) while the root mean square of sleep spindles was only significantly decreased in

central electrodes (C3/C4) but not in frontal cortex electrodes (F3/F4) (Figure 2C). Parallel to the decreased sleep spindle density, we observed similar brain-wide reductions in slow oscillations (Figure 3A-D) and K-complexes in individuals with early-stage ALS (Supplementary Figure 1). These results were not modified if individuals with intermediate AHI (5<AHI<20) and/or PMLSI (25<PMLSI<50) values were excluded from the analysis (Supplementary Figure 2). These observations indicate that sleep microarchitecture is disrupted across the entire brain in patients with early-stage ALS.

Presymptomatic ALS gene carriers show decreased sleep spindle density.

To further characterise the changes in the microarchitecture of sleep and to assess their onset during the course of the disease, a second prospective cohort study was conducted comprising presymptomatic ALS gene carriers, using identical inclusion and exclusion criteria (Figure 1B). This cohort corresponds to the cohort previously described in (13), with an additional 29 gene carriers and 11 first-degree relatives of fALS patients with negative genetic reports. A total of 57 presymptomatic gene carriers (*SOD1* n=13; *C9ORF72* n=33, remaining subjects: other mutations) and a total of 30 first-degree relatives without mutations were included in the analysis (Table 2). Here again, we did not identify patients or subjects with REM behaviour disorder that has been observed in prodromal neurodegenerative diseases. In the analysis, we focused on the two groups of *SOD1* gene carriers and *C9ORF72* gene carriers. The other mutation carriers were not analysed due to small sample size and heterogeneity.

Similarly to ALS patients, presymptomatic *SOD1* and *C9ORF72* ALS gene carriers demonstrated comparable reductions in sleep spindle density and root mean square (Figure 4A-B), with unchanged mean brain-wide amplitude (Figure 4B). The density and root mean square of sleep spindles were decreased in both *SOD1* and *C9ORF72* gene carriers in both frontal and central electrodes (Figure 4C). Interestingly, *SOD1*, but not *C9ORF72*, gene

carriers also displayed a mildly decreased amplitude of sleep spindle density in frontal and central areas (Figure 4C). A brain-wide reduction in slow oscillations (Figure 5) and K-complexes (Supplementary Figure 3) was observed in presymptomatic gene carriers, similar to that observed in patients with ALS. As in ALS patients, these results were not modified if individuals with intermediate AHI (5<AHI<20) and/or PMLSI (25<PMLSI<50) values were excluded from the analysis (Supplementary Figure 4). Thus, sleep microarchitecture is significantly impacted in ALS gene carriers who do not yet exhibit any signs of manifest disease.

Microarchitectural alterations of sleep patterns correlate with cognitive deficits.

Previous research demonstrated a correlation between modifications in the microarchitecture of sleep and the presence of cognitive deficits (14, 16). Furthermore, there is a link between sleep spindles and motor memory consolidation (18). To determine whether this association is also observed in our two cohorts, we correlated sleep microarchitecture parameters with cognitive function in both ALS patients and presymptomatic gene carriers, as well as with motor function in ALS patients. Cognitive function was evaluated using the Edinburgh Cognitive and Behavioural ALS Screen (ECAS) and motor function with the revised ALS functional rating scale (ALS-FRSr). In ALS patients, cognitive testing was conducted one to seven days after polysomnography in 58.5% of participants. 13.2% underwent the ECAS test the day before polysomnography, and 26.4% were tested the following day. In the presymptomatic gene carrier cohort, ECAS was always administered in the morning after polysomnography. ALS-FRSr was recorded between four days before and seven days after the sleep study.

In ALS patients, a significant positive correlation after adjustment for multiple comparisons was observed between total ECAS scores and either sleep spindle density or slow oscillation density (Figure 6A-C). We also observed significant correlations between densities of sleep

spindles or slow oscillation and various ECAS subscores (Figure 6A, Supplementary Figure 5-6, Supplementary Table 1) including memory, language function and verbal fluency subscores but not ALS-FRS-R score or its slope (Figure 6A, Supplementary Figure 5-6). In these patients, the correlations between cognitive assessment scores and K-complexes were noticeably weaker (Figure 6A, Supplementary Figure 7). In presymptomatic gene carriers, densities of sleep spindles or slow oscillation correlated also with total ECAS scores (Figure 6D-F, Supplementary Table 2) and well as several ECAS subscores (Figure 6D-F, Supplementary Figures 8-9), while there were no correlations with K-complexes (Supplementary Figure 10). Thus, the present findings indicate that alterations in the sleep microarchitecture are associated with cognitive performance, particularly in relation to verbal fluency, language function and memory.

Three ALS models exhibit microarchitectural alterations of sleep patterns.

Given the presence of sleep microarchitecture alterations in both early ALS patients and presymptomatic gene carriers, we sought to investigate whether these microarchitectural alterations are mirrored by findings in transgenic ALS mouse models. We studied three models expressing distinct ALS-causing mutations, each with markedly disparate disease progression and different genetic backgrounds. The transgenic model *Sod1*^{G86R} (in FVB/N genetic background) is associated with severe and rapidly progressive motor symptoms (19, 20), whereas the *Fus*$^{\Delta NLS/+}$ (21, 22) or *TDP-43*^{Q331K} models (in C57BL/6 background) (23) are linked to a light-to-mild and late-onset phenotype (13). We used datasets previously acquired (13) in mouse cohorts implanted with intracortical electrodes, focusing on recordings taken during the presymptomatic phase. In parallel to our findings in ALS patients and gene carriers, all three models demonstrated substantial alterations in sleep spindles (Figure 7A-E, Supplementary Figure 11). It is noteworthy that there was a significant decrease in sleep spindle density in 3-month-old *Fus*$^{\Delta NLS/+}$ mice (Figure 7C), despite showing no detectable alterations in sleep

macroarchitecture at this stage (13). As in ALS patients and presymptomatic gene carriers, decreased sleep spindle density in all three mouse models was also accompanied by decreased densities in both slow oscillations (Figure 7F-I) and K-complexes (Supplementary Figure 12). In all three models, microarchitectural alterations were consistently observed in both males and females. Thus, early changes in sleep microarchitecture are present in multiple ALS mouse models, mirroring alterations observed in early-stage ALS patients and presymptomatic gene carriers.

Sleep spindle defects are rescued by an orexin antagonist.

We previously showed that sleep alterations in ALS mouse models can be fully rescued through administration of suvorexant, a dual orexin receptor antagonist. We re-analysed the previous datasets in which Suvorexant or its vehicle was administered orally at the onset of the inactive period (*i.e.* during the day in mice). Single administration of Suvorexant increased sleep spindle density in all three mouse models near to wild-type levels, with a more pronounced effect in females, whereas efficacy was diminished in aged 10-month-old mice (Figure 8, Supplementary Figure 13). Similar restorative effects were observed for slow oscillations and K complexes (Supplementary Figure 14). MCH supplementation had similar, yet blunted effects on all sleep microarchitecture events in both *Sod1*^{G86R} mice (Supplementary Figure 15) and *Fus*$^{\Delta NLS/+}$ mice (Supplementary Figure 16). In all, our results suggest that increased orexinergic tone is causally related to sleep microarchitectural defects in both ALS mouse models and patients.

Discussion

In this study, we demonstrate that the disruption of sleep microarchitecture in ALS is profound, brain-wide and precedes the onset of motor symptoms in both humans and mouse models.

Alterations in sleep microarchitecture in ALS affect multiple sleep-related EEG features, including sleep spindles, slow oscillations and K-complexes. In ALS patients without respiratory impairment, as well as in presymptomatic ALS gene carriers, we observed reduced densities for all three EEG signals compared to their respective controls. The decrease in density was brain-wide, and we did not observe disruption patterns confined to isolated central or frontal regions. We also observed similar alterations in sleep microarchitecture in three mouse models of ALS. These defects in microarchitecture were more pronounced and appeared earlier in mouse models than macroarchitectural abnormalities (13). Indeed, while we previously did not observe increased wakefulness or decreased NREM at three months of age in *Fus*$^{\Delta NLS/+}$ mice, there was a loss of sleep spindles, slow oscillations and K-complexes at this age. These findings have to be confirmed in patients with *FUS* mutations but could be used as among the earliest detectable changes in ALS pathophysiology as they precede other symptomatic and sleep macroarchitecture alterations observed in that particular mutation.

Disruption of sleep EEG features, as we describe here in ALS, is widely observed in neurological and neurodegenerative diseases. Loss of sleep spindles, particularly decreased density, and of slow oscillations, has been consistently observed in Alzheimer's disease (24-26) or Parkinson's disease (27-29), and in other neurological diseases such as temporal lobe epilepsy (30), schizophrenia (31-33). Remarkably, this was not observed in patients with ADHD, PTSD or most patients with autism spectrum disorder (31). Sleep spindle density also decreases with age (34), suggesting that accelerated brain ageing could account for some of our results in ALS patients, both in terms of microarchitecture defects (the current study) or

for macroarchitecture changes (13). Furthermore, as decreased sleep spindle density is observed in several neurological and neurodegenerative conditions, the current observation is unlikely to be used as diagnostic. Nevertheless, sleep spindles and slow oscillations are quantifiable parameters, and their disruption appears early, in the prodromal stage of the disease. Therefore, it is reasonable to hypothesise that sleep electroencephalograms (EEGs) may contain hallmarks that could be explored for prognostic purposes.

There are two limitations of our current description of sleep microarchitecture defects. First, we present evidence of presymptomatic defects only in familial ALS (fALS), both in presymptomatic gene carriers and in mouse models. We do not have access to prediagnostic polysomnography in sporadic ALS (sALS), and can only assume that our observation in fALS extends to sALS. Second, our current study is cross-sectional and lacks longitudinal follow-up. Consequently, we are currently unable to determine whether these phenotypes worsen as symptom onset approaches or with disease progression. Future studies should include longitudinal polysomnography in presymptomatic gene carriers to determine the dynamics of sleep macro- and micro-architecture and their possible role as prognostic markers of phenoconversion.

What might be the consequences of defects in sleep microarchitecture? It has been documented that sleep spindles and slow oscillations are causally involved in memory consolidation and executive functions (14, 16). In patients with Parkinson's or Alzheimer's diseases, the severity of sleep spindle disruption has been linked to memory and cognitive impairments (24-29). Complementing these findings, we observed strong correlations between cognitive scores and sleep spindles and slow oscillations in our two cohorts. These correlations were stronger than previously reported associations between sleep stages and cognitive function in the same cohorts (13). Whether loss of sleep spindles affects motor progression in ALS remains unknown. Notably, sleep spindles are highly associated with

motor adaptation (35) and motor memory consolidation (18, 36-39), and disruption of this functional balance could potentially accelerate or exacerbate motor decline. Longitudinal studies in patients and gene carriers, as well as experimental rodent studies, may help address this question.

Defects in sleep microarchitecture may arise from multiple causes, which our study does not definitively distinguish. First, defects in intra-cortical circuits could impair slow oscillations, sleep spindles and K-complexes, as these EEG patterns originate and propagate locally within cortical networks, and particularly the frontal part (40-45). In this context impaired frontal lobe function in ALS (46, 47) may contribute to the abnormalities observed. Second, these defects could result from dysfunction in subcortical structures such as the thalamus. Sleep spindles originate in the thalamus (14, 16), which also plays a key role in modulating the timing, coherence and spindle nesting of slow oscillations (48, 49). Thalamic atrophy has been documented in ALS, particularly in *C9ORF72* patients (50-55), and alterations of the thalamo-cortical pathway have been observed in both sporadic ALS (56, 57) and presymptomatic *C9ORF72* gene carriers (58). These thalamic alterations have been linked to faster progression in sporadic ALS (59) and higher risk of phenoconversion in *C9ORF72* ALS (60). Thalamic involvement is considered an early biomarker of ALS, contributing to both motor and cognitive deficits in sporadic cases (61-64), and is described as an early event, stage 2 in the Braak staging system of TDP-43 pathology spread (65, 66). Third, impairments in monoaminergic pathways, particularly acetylcholine (67-70) or norepinephrine (71-73) could be the origin of sleep microarchitecture alterations. This would align with previous observations of acetylcholine defects (70) or norepinephrine (74) dysfunction in ALS. Finally, part of the observed microarchitectural changes may be caused by hypothalamic defects, such as orexin or MCH signalling alterations. Our results show that orexin antagonism or MCH supplementation can rescue the loss of sleep spindles and slow oscillations in several ALS

mouse models, strongly implicating the hypothalamus. This aligns with reported MCH neuron loss in ALS postmortem tissues (75), and several studies indicating orexin pathway alterations in ALS patients and mouse models (13, 76, 77). These mechanisms are not mutually exclusive as thalamic reticular nucleus neurons are sensitive to orexin (78, 79), and are also highly modulated by cholinergic or noradrenergic innervation during sleep (72, 80-82). Our findings do not establish a direct causal relationship between MCH/orexin signalling and microarchitecture sleep defects. It remains possible that sleep dysfunctions originate in other brain regions such as the cortex, locus coeruleus or thalamus, and are corrected by MCH or suvorexant. Elucidating the mechanisms behind sleep microarchitecture defects will require further experimental investigation.

In summary, our study identifies alterations in sleep EEG as an early biomarker of ALS, detectable many years before symptom onset in presymptomatic gene carriers and correlates with cognitive decline. Uncovering the underlying mechanisms may offer critical insights into the earliest pathophysiological events in ALS. Further longitudinal studies are needed to evaluate whether sleep microarchitecture alterations can serve as prognostic markers for phenoconversion and disease progression, especially given its easy set-up in clinical pratice. Preclinical evaluation of chronic administration of dual orexin receptor antagonists is now required to determine its safety in ALS models, and its potential translational relevance for improving sleep, mitigating cognitive deficits, preventing weight loss and slowing motor symptom progression, ultimately justifying future human clinical trials.

Methods

Sex as a biological variable

Our study involved both male and female subjects, both for human studies and experimental mouse models. Sex is indicated on each figure and was considered a biological variable for statistical analysis. The effect of sex is reported in the figure legends.

Patients and participants.

ALS patients were recruited from the inpatient and outpatient clinics of the Neurology Department of the University Hospital of Ulm, Germany. The inclusion criteria for ALS patients included a diagnosis of definite ALS based on the revised El Escorial criteria (83). Presymptomatic carriers of fALS genes were recruited through the study centre of the University Neurology Clinic, which provides longitudinal follow-up and counselling to first-degree relatives of confirmed familial ALS patients. Controls were recruited from the general population of the Neurology Clinic, and were matched to ALS patients based on age, sex, and geographical location; the requirement for this group was the exclusion of neurodegenerative diseases. All individuals in the control group were unrelated to ALS or familial ALS.

Medical history was documented. For ALS patients, the ALSFRS-r and characteristics of disease progression were documented (site of first paresis/atrophy, date of onset). All participants also completed validated daytime sleepiness and sleep quality questionnaires, namely the Epworth Sleepiness Scale (ESS) (84) and the Pittsburgh Sleep Quality Index (PSQI) (85). The current medication of all participants was documented, and no exclusion criteria related to medication use were applied that would have prevented participation.

Patients' inclusion process.

The same exclusion criteria employed by Guillot SJ et al. (13) were applied and summarised in Figure 1. Participation in the study was possible in this cohort for both sporadic patients and

familial ALS patients. Exclusion criteria were designed to exclude all possible circumstances that might otherwise alter sleep architecture. For this reason, participants who had an apnoea-hypopnea index (AHI) above 20 per hour or participants who had a periodic limb movement index (PLMSI) above 50 per hour were excluded. In particular, we intended to exclude respiratory insufficiency in ALS patients. Respiratory insufficiency develops earlier or later in the progression of ALS, depending on the individual course, but is generally present in advanced stages and is known to influence sleep architecture (86). For this reason, ALS patients received transcutaneous capnometry in addition to polysomnography. Capnometry results had to be normal or nocturnal hypercapnia would result in exclusion from the study.

Inclusion process of first-degree relatives of fALS patients.

The same exclusion criteria employed by Guillot SJ et al (13) were followed. We enrolled first-degree relatives of fALS patients in whom the ALS-causing mutation is known. The participants were examined according to the study protocol and genotyping was also performed. Neither the participants nor the study personnel were informed of the genetic results at the time of the examinations. After the study visits, participants were assigned to the group of presymptomatic gene carriers or the control group with negative genetic findings based on their genetic results. The participants could only learn the result of the genetic test if they had completed the legally required genetic counselling appointments (according to the German Genetic Diagnostics Act).

Neuropsychological Assessment

Cognition was measured with the German version of the Edinburgh Cognitive and Behavioural ALS Screen (ECAS) (87-89) by trained neuropsychologists. The ECAS addresses cognitive domains of language function, verbal fluency, executive functions (ALS-specific functions) and memory and visuospatial functions (ALS non-specific functions). Age and education-adjusted

cut-offs were used (89). Behavioural changes were assessed by patient caregiver/first-degree relative interviews on disinhibition, apathy, loss of sympathy/empathy, perseverative/stereotyped behaviour, hyperorality/altered eating behaviour and psychotic symptoms. Since the participants in the ALS patient cohort were hospitalised, the neuropsychological examination was conducted in the days before or after the polysomnography, with a maximum interval of one week. The participants of the presymptomatic gene carrier cohort underwent the neuropsychological examination the morning after the polysomnography.

Electroencephalography in patients and subjects.

All participants —ALS patients, healthy individuals, presymptomatic fALS gene carriers, and fALS control individuals— underwent a one-night full polysomnography, which was performed in the inpatient sleep laboratory of the Deparment of Neurology at Ulm University Hospital, involving monitoring of various physiological parameters including electroencephalogram (EEG), surface electromyogram (EMG), electrooculogram (EOG), respiratory effort and flow, pulse and oxygen saturation. To minimise bias, conditions were standardised within each cohort: presymptomatic gene carriers followed a protocol with arrival in the morning, polysomnography at night, neuropsychology the next day and ALS patients with their controls underwent polysomnography during a single night of a multi-day inpatient stay. All measurements were conducted according to the criteria of the American Academy of Sleep Medicine (AASM) guidelines (90, 91). The EEG electrodes were placed according to the international 10-20 system. The following electrodes were used in each subject: Fz, C3, C4, Cz, P3, P4, Pz, O1, O2, M1, and M2. The sampling rate was 512 Hz in each case. The EEG montage was in accordance with the general recommendation of the AASM guideline, with contralateral referencing to the mastoid electrode, i.e. F3-M2, C3-M2, O1-M2, and F4-M1, C4-M1, O2-M1. A "lights off" marker was placed in each recording to indicate the individual point

in time when the participant turned off the lights and attempted to sleep. In order to accommodate sleep times as closely as possible to the chronotype, participants were allowed to choose the start time of the examination freely, but the latest time was midnight. The occurrence of REM Sleep behaviour disorder was evaluated in all individuals using previously defined criteria (17).

Sleep analyses in patients and subjects.

Analyses were performed using available Python packages (only compatible with Python 3.10 or newer, Python Software Foundation. Python Language Reference, version 3.12. Available at http://www.python.org) relying on MNE package (92). EEGs preprocessing was performed following Guillot SJ et al (13).

Briefly, recordings were first de-identified using the open-source Prerau Lab EDF De-identification Tool (Version 1.0; 2023) in Python (Prerau Lab EDF De-identification Tool retrieved from https://sleepeeg.org/edf-de-identification-tool), to then be notch-filtered to remove the 50Hz powerline. Independent component analysis was performed to remove all remaining artefacts from the signal (93-97).

Analyses of sleep spindles, slow oscillations and K-complexes were performed on all electrodes (41, 98, 99) and outliers were removed using an isolation forest algorithm (100). K-complex analysis was limited to the sensorimotor cortex (C3), which is known to be impaired in ALS, using MNE and SciPy packages (100, 101). For the sleep spindles, their density (number of sleep spindles per minute of NREM2/3 sleep), amplitude (peak-to-peak amplitude of the detrended sleep spindle) and root-mean-square (RMS) with the frequency bands set to 12-15Hz and required to last 0.5-2sec. For the slow oscillation, its density (number of slow oscillations per minute of NREM2/3), slope (slope between the negative peak and the midpoint of the slow oscillation), phase-amplitude coupling (PAC; slow oscillations-sleep spindles normalised PAC within a 2sec epoch centred around the negative peak of the slow oscillation)

and phase at sigma peak (phase of the slow oscillation when the sigma peak is reached within a 2-second epoch centered around the negative peak of the slow oscillation) were analysed, with the frequency bands set to 0.3-1.5Hz and amplitude below 150μV. For the K-complex assessment, we analysed its density (number of K-complexes per minute of NREM2), with the frequency bands set to 0.3-1Hz and amplitude between 100-350μV. Topographic maps were performed using MNE and YASA packages (102). All analyses were performed following the AASM's guidelines (103).

Electrocorticography analysis in mice.

Data were extracted from the NeuroScore™ software for sleep and seizure analysis 3.4 (Data Science International Inc., St. Paul, MN, USA) and used in combination with already available Python packages (Python Software Foundation. Python Language Reference, version 3.12. Available at http://www.python.org) to further process the data.

Sleep spindles, slow oscillations and K-complexes were automatically detected using publicly available pipelines(104, 105). The signal was first band-pass filtered at 1-45Hz, and the sigma power (12-16Hz) was calculated on a 200ms Hamming window followed by a Short-Term Fourier Transform (STFT) with the same window length. The occurrence of sleep spindles was identified when the smoothed absolute sigma power within the 12-16 Hz range exceeded 0.2 of the total power observed in the broadband frequency range of 0.1-45Hz. This signifies that at least 20% of the total signal power must be within the specified sigma band.

$$P_{rel\sigma}(dB) = \log_{10}\left(\frac{\int_{11}^{16}|x(t)|^2\,dt}{\int_{0.1}^{45}|x(t)|^2\,dt}\right) \times \log_{10}\left(\frac{\int_{11}^{16}|x(t)|^2\,dt}{\int_{0.1}^{45}|x(t)|^2\,dt}\right)$$

For slow oscillations, the signal was first band-pass filtered at 0.1-45Hz, and the low delta power (0.1-2Hz) was calculated on a 400ms Hamming window. Areas under the curve (AUC) were calculated using Simpson's rule derived from the delta band (A_{SO}) and the total power

broadband frequency range (B_{PSD}). The ratio of these two AUCs was then obtained, providing the slow oscillations ratio.

$$\mathrm{C}_{ratio} = \frac{\mathrm{A}_{SO}}{\mathrm{B}_{PSD}} = \frac{\int_{0.1}^{2} f(x)dx}{\int_{0.1}^{45} f(x)dx}$$

For K-complexes, the signal was first band-pass filtered at 0.1-45Hz, and the sigma power was calculated on a 400ms Hamming window. The signal was first band-pass filtered at 1-45Hz, and the low delta power (0.3-1Hz) was calculated on a 200ms Hamming window followed by an STFT with the same window length. The occurrence of K-complexes was identified when the STFT within the 0.3-1Hz range exceeded the mean STFT of the same frequency range.

$$\int_{0.3}^{1} STFT_{(x(t))(\tau,\omega)} \geq \int_{0.3}^{1} \overline{STFT}$$

$$\text{where } \mathrm{STFT}_{(x(t))(\tau,\omega)} \equiv X(\tau,\omega) = \int_{0.3}^{1} x(t)\omega(t-\tau)e^{-i\omega t}\,dt$$

Statistical analyses.

G*Power software (Version 3.1.9.6 for macOS; 2023) was used to determine the sufficient sample size needed to achieve significant statistical power using an *a priori* Student's t-test coupled with a linear bivariate regression (106, 107).

Prior to any statistical analysis, normality and homoscedasticity were both tested respectively with Shapiro-Wilk test (108) and Bartlett's test (109).

For comparisons between two groups, an independent Student's t-test was performed using Pingouin(110), with the Welch's t-test correction, from SciPy, as recommended by Zimmerman (111). A large Cauchy scale factor was incorporated due to the considerate effect size (112). When data violated normality or heteroscedastic a Mann-Whitney *U* test was performed using SciPy (100).

Follow-up analyses were performed using a paired t-test from SciPy (100) or a Wilcoxon-Mann-Whitney rank-sum test from statsmodels (113) when normality was not met. P_{values} were then adjusted using FDR-BKY correction.

For comparisons among three or four groups, a One-way ANOVA or Two-way ANOVA was performed using the Pingouin (110) toolbox. For both ANOVA models, a multiple comparison test with FDR-BKY correction was applied. If normality or heteroscedastic assumptions were not met, a Kruskal-Wallis test from SciPy (100) followed by Dunn's multiple comparison test with FDR-BKY correction was performed using scikit-posthocs (114). instead of a One-Way ANOVA. For the Two-Way ANOVA, a generalised least squares model was fitted using statsmodels (113), followed by Dunn's multiple comparison and FDR-BKY correction using scikit-posthocs (114). We evaluated whether a sex-specific effect was present in all our analyses by performing a Two-way ANOVA with a multiple comparison test with FDR-BKY correction for both sexes. Sex was self-reported in both ALS cohorts.

Spearman's correlation coefficient from SciPy (100), was used for correlations on non-parametric data.

Data are presented as violin plots with all points and expressed as medians ± interquartile range. Visualisations were generated using Seaborn and Matplotlib packages (115). Results were deemed significant when at adjusted $p_{value}<0.05$. Here, only corrected p_{values} (adj. p_{value}) are shown.

Study approval

The study in the ALS patient cohort was approved by the Ethics Committee of the University of Ulm (reference 391/18). The study in presymptomatic carriers received approval by the same Ethics Committee of the University of Ulm (reference 68/19), in accordance with the ethical standards of the current version of the revised Helsinki Declaration. All participants provided written informed consent prior to enrollment.

Mouse experiments were performed in full compliance with Directive 2010/63/EU, and new Regulation (EU) 2019/1010, and the project was reviewed and approved by the Ethics Committee of the University of Strasbourg and the French Ministry of Higher Education, Research and Innovation (Decree n°2013-118, February 1st, 2013). All procedures including animal care, surgery and datasets used in this study have been previously described in (13).

Data availability

Additional data are available upon request to the corresponding authors. All numerical data are provided in supporting data file.

Author contributions

CL, SJG, ACL, MB and LD conceptualized the study. CL, SJG, DL, LTB, AK, PW, JD, KK, HPM, JK, LW, MB performed the investigation. CL, SJG, ACL, MB, LD analyzed the results. CL, SJG, LD generated vizualization of results. SJG, SDC, ACL, MB, LD provided resources. ACL, FR, LD acquired fundings. AK, PW, JD, FR, ACL, MB, LD were involved in project administration. ACL, MB, LD supervised the project. CL, SJG, MB, LD wrote original draft, and all authors reviewed, edited and approved the manuscript.

Acknowledgments

The authors thank the patients and their families, as well as volunteers for their participation in these studies. The authors are thankful to the Animal Facility Core (PEFRE, University of Strasbourg, INSERM, UMS 38). Fondation Anne-Marie et Roger Dreyfus (hosted by Fondation de France) provided salary for SJG. CL was supported by a salary from the Charcot Stiftung. This work was funded by Agence Nationale de la Recherche (ANR-24-CE37-4064), the Interdisciplinary Thematic Institute NeuroStra, as part of the ITI 2021-2028 (Idex Unistra ANR-10-IDEX-0002, ANR-20-SFRI-0012), Fondation Thierry Latran, Association Francaise

de Recherche sur la sclérose latérale amyotrophique, Association Française contre les Myopathies (AFM-Téléthon, #28944), TargetALS and JPND (HiCALS project).

References

1. Goutman SA, Hardiman O, Al-Chalabi A, Chio A, Savelieff MG, Kiernan MC, and Feldman EL. Emerging insights into the complex genetics and pathophysiology of amyotrophic lateral sclerosis. *Lancet Neurol.* 2022.
2. Goutman SA, Hardiman O, Al-Chalabi A, Chio A, Savelieff MG, Kiernan MC, and Feldman EL. Recent advances in the diagnosis and prognosis of amyotrophic lateral sclerosis. *Lancet Neurol.* 2022.
3. Weydt P, Oeckl P, Huss A, Muller K, Volk AE, Kuhle J, Knehr A, Andersen PM, Prudlo J, Steinacker P, et al. Neurofilament levels as biomarkers in asymptomatic and symptomatic familial amyotrophic lateral sclerosis. *Ann Neurol.* 2016;79(1):152-8.
4. Benatar M, Granit V, Andersen PM, Grignon AL, McHutchison C, Cosentino S, Malaspina A, and Wuu J. Mild motor impairment as prodromal state in amyotrophic lateral sclerosis: a new diagnostic entity. *Brain.* 2022;145(10):3500-8.
5. Benatar M, Wuu J, Huey ED, McMillan CT, Petersen RC, Postuma R, McHutchison C, Dratch L, Arias JJ, Crawley A, et al. The Miami Framework for ALS and related neurodegenerative disorders: an integrated view of phenotype and biology. *Nat Rev Neurol.* 2024;20(6):364-76.
6. Diekmann K, Kuzma-Kozakiewicz M, Piotrkiewicz M, Gromicho M, Grosskreutz J, Andersen PM, de Carvalho M, Uysal H, Osmanovic A, Schreiber-Katz O, et al. Impact of comorbidities and co-medication on disease onset and progression in a large German ALS patient group. *J Neurol.* 2020;267(7):2130-41.
7. Janse van Mantgem MR, van Eijk RPA, van der Burgh HK, Tan HHG, Westeneng HJ, van Es MA, Veldink JH, and van den Berg LH. Prognostic value of weight loss in patients with amyotrophic lateral sclerosis: a population-based study. *J Neurol Neurosurg Psychiatry.* 2020;91(8):867-75.
8. Wei QQ, Ou R, Cao B, Chen Y, Hou Y, Zhang L, Wu F, and Shang H. Early weight instability is associated with cognitive decline and poor survival in amyotrophic lateral sclerosis. *Brain Res Bull.* 2021;171(10-5.
9. Li JY, Sun XH, Cai ZY, Shen DC, Yang XZ, Liu MS, and Cui LY. Correlation of weight and body composition with disease progression rate in patients with amyotrophic lateral sclerosis. *Sci Rep.* 2022;12(1):13292.
10. Peter RS, Rosenbohm A, Dupuis L, Brehme T, Kassubek J, Rothenbacher D, Nagel G, and Ludolph AC. Life course body mass index and risk and prognosis of amyotrophic lateral sclerosis: results from the ALS registry Swabia. *Eur J Epidemiol.* 2017;32(10):901-8.
11. Abrahams S. Neuropsychological impairment in amyotrophic lateral sclerosis-frontotemporal spectrum disorder. *Nat Rev Neurol.* 2023;19(11):655-67.
12. Lule DE, Muller HP, Finsel J, Weydt P, Knehr A, Winroth I, Andersen P, Weishaupt J, Uttner I, Kassubek J, et al. Deficits in verbal fluency in presymptomatic C9orf72 mutation gene carriers-a developmental disorder. *J Neurol Neurosurg Psychiatry.* 2020;91(11):1195-200.
13. Guillot SJ, Lang C, Simonot M, Beckett D, Lule D, Balz LT, Knehr A, Stuart-Lopez G, Vercruysse P, Dieterle S, et al. Early-onset sleep alterations found in

patients with amyotrophic lateral sclerosis are ameliorated by orexin antagonist in mouse models. *Sci Transl Med.* 2025;17(783):eadm7580.
14. Fernandez LMJ, and Luthi A. Sleep Spindles: Mechanisms and Functions. *Physiol Rev.* 2020;100(2):805-68.
15. Purcell SM, Manoach DS, Demanuele C, Cade BE, Mariani S, Cox R, Panagiotaropoulou G, Saxena R, Pan JQ, Smoller JW, et al. Characterizing sleep spindles in 11,630 individuals from the National Sleep Research Resource. *Nat Commun.* 2017;8(15930.
16. Brodt S, Inostroza M, Niethard N, and Born J. Sleep-A brain-state serving systems memory consolidation. *Neuron.* 2023;111(7):1050-75.
17. Mayer G, Kesper K, Ploch T, Canisius S, Penzel T, Oertel W, and Stiasny-Kolster K. Quantification of tonic and phasic muscle activity in REM sleep behavior disorder. *J Clin Neurophysiol.* 2008;25(1):48-55.
18. Baena D, Gabitov E, Ray LB, Doyon J, and Fogel SM. Motor learning promotes regionally-specific spindle-slow wave coupled cerebral memory reactivation. *Commun Biol.* 2024;7(1):1492.
19. Dupuis L, de Tapia M, Rene F, Lutz-Bucher B, Gordon JW, Mercken L, Pradier L, and Loeffler JP. Differential screening of mutated SOD1 transgenic mice reveals early up-regulation of a fast axonal transport component in spinal cord motor neurons. *Neurobiology of Disease.* 2000;7(4):274-85.
20. Dupuis L, Oudart H, Rene F, Gonzalez de Aguilar JL, and Loeffler JP. Evidence for defective energy homeostasis in amyotrophic lateral sclerosis: benefit of a high-energy diet in a transgenic mouse model. *Proc Natl Acad Sci U S A.* 2004;101(30):11159-64.
21. Scekic-Zahirovic J, Sendscheid O, El Oussini H, Jambeau M, Sun Y, Mersmann S, Wagner M, Dieterle S, Sinniger J, Dirrig-Grosch S, et al. Toxic gain of function from mutant FUS protein is crucial to trigger cell autonomous motor neuron loss. *EMBO J.* 2016;35(10):1077-97.
22. Scekic-Zahirovic J, El Oussini H, Mersmann S, Drenner K, Wagner M, Sun Y, Allmeroth K, Dieterle S, Sinniger J, Dirrig-Grosch S, et al. Motor neuron intrinsic and extrinsic mechanisms contribute to the pathogenesis of FUS-associated amyotrophic lateral sclerosis. *Acta Neuropathol (Berl).* 2017;133(6):887-906.
23. Arnold ES, Ling SC, Huelga SC, Lagier-Tourenne C, Polymenidou M, Ditsworth D, Kordasiewicz HB, McAlonis-Downes M, Platoshyn O, Parone PA, et al. ALS-linked TDP-43 mutations produce aberrant RNA splicing and adult-onset motor neuron disease without aggregation or loss of nuclear TDP-43. *Proc Natl Acad Sci U S A.* 2013.
24. Zhang Y, Ren R, Yang L, Zhang H, Shi Y, Okhravi HR, Vitiello MV, Sanford LD, and Tang X. Sleep in Alzheimer's disease: a systematic review and meta-analysis of polysomnographic findings. *Transl Psychiatry.* 2022;12(1):136.
25. D'Rozario AL, Chapman JL, Phillips CL, Palmer JR, Hoyos CM, Mowszowski L, Duffy SL, Marshall NS, Benca R, Mander B, et al. Objective measurement of sleep in mild cognitive impairment: A systematic review and meta-analysis. *Sleep Med Rev.* 2020;52(101308.
26. Weng YY, Lei X, and Yu J. Sleep spindle abnormalities related to Alzheimer's disease: a systematic mini-review. *Sleep Med.* 2020;75(37-44.
27. Villamar-Flores CI, Rodriguez-Violante M, Abundes-Corona A, Alatriste-Booth V, Valencia-Flores M, Rodriguez-Agudelo Y, Cervantes-Arriaga A, and Solis-

Vivanco R. Association between alterations in sleep spindles and cognitive decline in persons with Parkinson's disease. *Neuroscience letters.* 2024;842(138006.
28. Latreille V, Carrier J, Gaudet-Fex B, Rodrigues-Brazete J, Panisset M, Chouinard S, Postuma RB, and Gagnon JF. Electroencephalographic prodromal markers of dementia across conscious states in Parkinson's disease. *Brain.* 2016;139(Pt 4):1189-99.
29. Christensen JA, Nikolic M, Warby SC, Koch H, Zoetmulder M, Frandsen R, Moghadam KK, Sorensen HB, Mignot E, and Jennum PJ. Sleep spindle alterations in patients with Parkinson's disease. *Front Hum Neurosci.* 2015;9(233.
30. Bender AC, Jaleel A, Pellerin KR, Moguilner S, Sarkis RA, Cash SS, and Lam AD. Altered Sleep Microarchitecture and Cognitive Impairment in Patients With Temporal Lobe Epilepsy. *Neurology.* 2023;101(23):e2376-e87.
31. Mayeli A, Sanguineti C, and Ferrarelli F. Recent Evidence of Non-Rapid Eye Movement Sleep Oscillation Abnormalities in Psychiatric Disorders. *Curr Psychiatry Rep.* 2024.
32. Denis D, Baran B, Mylonas D, Spitzer C, Raymond N, Talbot C, Kohnke E, Larson O, Stickgold R, Keshavan M, et al. Sleep oscillations and their relations with sleep-dependent memory consolidation in early course psychosis and first-degree relatives. *Schizophr Res.* 2024;274(473-85.
33. Ferrarelli F. Sleep spindles as neurophysiological biomarkers of schizophrenia. *Eur J Neurosci.* 2024;59(8):1907-17.
34. Peters KR, Ray LB, Fogel S, Smith V, and Smith CT. Age differences in the variability and distribution of sleep spindle and rapid eye movement densities. *PLoS One.* 2014;9(3):e91047.
35. Ameen MS, Petzka M, Peigneux P, and Hoedlmoser K. Post-training sleep modulates motor adaptation and task-related beta oscillations. *J Sleep Res.* 2024;33(4):e14082.
36. Hahn MA, Bothe K, Heib D, Schabus M, Helfrich RF, and Hoedlmoser K. Slow oscillation-spindle coupling strength predicts real-life gross-motor learning in adolescents and adults. *eLife.* 2022;11(
37. Boutin A, and Doyon J. A sleep spindle framework for motor memory consolidation. *Philos Trans R Soc Lond B Biol Sci.* 2020;375(1799):20190232.
38. Kam K, Pettibone WD, Shim K, Chen RK, and Varga AW. Dynamics of sleep spindles and coupling to slow oscillations following motor learning in adult mice. *Neurobiol Learn Mem.* 2019;166(107100.
39. Laventure S, Fogel S, Lungu O, Albouy G, Sevigny-Dupont P, Vien C, Sayour C, Carrier J, Benali H, and Doyon J. NREM2 and Sleep Spindles Are Instrumental to the Consolidation of Motor Sequence Memories. *PLoS biology.* 2016;14(3):e1002429.
40. Covelo J, Camassa A, Sanchez-Sanchez JM, Manasanch A, Porta LD, Cancino-Fuentes N, Barbero-Castillo A, Robles RM, Bosch M, Tapia-Gonzalez S, et al. Spatiotemporal network dynamics and structural correlates in the human cerebral cortex in vitro. *Prog Neurobiol.* 2025;246(102719.
41. Massimini M, Huber R, Ferrarelli F, Hill S, and Tononi G. The sleep slow oscillation as a traveling wave. *J Neurosci.* 2004;24(31):6862-70.

42. Nir Y, Staba RJ, Andrillon T, Vyazovskiy VV, Cirelli C, Fried I, and Tononi G. Regional slow waves and spindles in human sleep. *Neuron.* 2011;70(1):153-69.
43. Girardeau G, and Lopes-Dos-Santos V. Brain neural patterns and the memory function of sleep. *Science.* 2021;374(6567):560-4.
44. Amzica F, and Steriade M. The K-complex: its slow (<1-Hz) rhythmicity and relation to delta waves. *Neurology.* 1997;49(4):952-9.
45. Halasz P. The K-complex as a special reactive sleep slow wave - A theoretical update. *Sleep Med Rev.* 2016;29(34-40.
46. Mohammadi B, Kollewe K, Cole DM, Fellbrich A, Heldmann M, Samii A, Dengler R, Petri S, Munte TF, and Kramer UM. Amyotrophic lateral sclerosis affects cortical and subcortical activity underlying motor inhibition and action monitoring. *Hum Brain Mapp.* 2015;36(8):2878-89.
47. Metzger M, Dukic S, McMackin R, Giglia E, Mitchell M, Bista S, Costello E, Peelo C, Tadjine Y, Sirenko V, et al. Distinct Longitudinal Changes in EEG Measures Reflecting Functional Network Disruption in ALS Cognitive Phenotypes. *Brain Topogr.* 2024;38(1):3.
48. Crunelli V, David F, Lorincz ML, and Hughes SW. The thalamocortical network as a single slow wave-generating unit. *Curr Opin Neurobiol.* 2015;31(72-80.
49. Neske GT. The Slow Oscillation in Cortical and Thalamic Networks: Mechanisms and Functions. *Front Neural Circuits.* 2015;9(88.
50. Wiesenfarth M, Huppertz HJ, Dorst J, Lule D, Ludolph AC, Muller HP, and Kassubek J. Structural and microstructural neuroimaging signature of C9orf72-associated ALS: A multiparametric MRI study. *Neuroimage Clin.* 2023;39(103505.
51. Nigri A, Umberto M, Stanziano M, Ferraro S, Fedeli D, Medina Carrion JP, Palermo S, Lequio L, Denegri F, Agosta F, et al. C9orf72 ALS mutation carriers show extensive cortical and subcortical damage compared to matched wild-type ALS patients. *Neuroimage Clin.* 2023;38(103400.
52. Bonham LW, Geier EG, Sirkis DW, Leong JK, Ramos EM, Wang Q, Karydas A, Lee SE, Sturm VE, Sawyer RP, et al. Radiogenomics of C9orf72 Expansion Carriers Reveals Global Transposable Element Derepression and Enables Prediction of Thalamic Atrophy and Clinical Impairment. *J Neurosci.* 2023;43(2):333-45.
53. Chipika RH, Siah WF, Shing SLH, Finegan E, McKenna MC, Christidi F, Chang KM, Karavasilis E, Vajda A, Hengeveld JC, et al. MRI data confirm the selective involvement of thalamic and amygdalar nuclei in amyotrophic lateral sclerosis and primary lateral sclerosis. *Data Brief.* 2020;32(106246.
54. Schonecker S, Neuhofer C, Otto M, Ludolph A, Kassubek J, Landwehrmeyer B, Anderl-Straub S, Semler E, Diehl-Schmid J, Prix C, et al. Atrophy in the Thalamus But Not Cerebellum Is Specific for C9orf72 FTD and ALS Patients - An Atlas-Based Volumetric MRI Study. *Front Aging Neurosci.* 2018;10(45.
55. Westeneng HJ, Walhout R, Straathof M, Schmidt R, Hendrikse J, Veldink JH, van den Heuvel MP, and van den Berg LH. Widespread structural brain involvement in ALS is not limited to the C9orf72 repeat expansion. *J Neurol Neurosurg Psychiatry.* 2016;87(12):1354-60.

56. Zhang JQ, Ji B, Zhou CY, Li LC, Li ZH, Hu XP, and Hu J. Differential Impairment of Thalamocortical Structural Connectivity in Amyotrophic Lateral Sclerosis. *CNS Neurosci Ther.* 2017;23(2):155-61.
57. Lee SE, Khazenzon AM, Trujillo AJ, Guo CC, Yokoyama JS, Sha SJ, Takada LT, Karydas AM, Block NR, Coppola G, et al. Altered network connectivity in frontotemporal dementia with C9orf72 hexanucleotide repeat expansion. *Brain.* 2014;137(Pt 11):3047-60.
58. Shoukry RS, Waugh R, Bartlett D, Raitcheva D, and Floeter MK. Longitudinal changes in resting state networks in early presymptomatic carriers of C9orf72 expansions. *Neuroimage Clin.* 2020;28(102354.
59. Lajoie I, Canadian ALSNC, Kalra S, and Dadar M. Regional Cerebral Atrophy Contributes to Personalized Survival Prediction in Amyotrophic Lateral Sclerosis: A Multicentre, Machine Learning, Deformation-Based Morphometry Study. *Ann Neurol.* 2025.
60. van Veenhuijzen K, Tan HHG, Nitert AD, van Es MA, Veldink JH, van den Berg LH, and Westeneng HJ. Longitudinal Magnetic Resonance Imaging in Asymptomatic C9orf72 Mutation Carriers Distinguishes Phenoconverters to Amyotrophic Lateral Sclerosis or Amyotrophic Lateral Sclerosis With Frontotemporal Dementia. *Ann Neurol.* 2025;97(2):281-95.
61. Mohammadi S, Ghaderi S, Mohammadi M, Najafi Asli Pashaki Z, Khatyal R, Mohammadian F, and Mohammadjani S. Thalamic Alterations in Motor Neuron Diseases: A Systematic Review of MRI Findings. *J Integr Neurosci.* 2024;23(4):77.
62. Hinault T, Segobin S, Benbrika S, Carluer L, Doidy F, Eustache F, Viader F, and Desgranges B. Longitudinal grey matter and metabolic contributions to cognitive changes in amyotrophic lateral sclerosis. *Brain Commun.* 2022;4(5):fcac228.
63. Machts J, Loewe K, Kaufmann J, Jakubiczka S, Abdulla S, Petri S, Dengler R, Heinze HJ, Vielhaber S, Schoenfeld MA, et al. Basal ganglia pathology in ALS is associated with neuropsychological deficits. *Neurology.* 2015;85(15):1301-9.
64. Tu S, Menke RAL, Talbot K, Kiernan MC, and Turner MR. Regional thalamic MRI as a marker of widespread cortical pathology and progressive frontotemporal involvement in amyotrophic lateral sclerosis. *J Neurol Neurosurg Psychiatry.* 2018;89(12):1250-8.
65. Braak H, Brettschneider J, Ludolph AC, Lee VM, Trojanowski JQ, and Del Tredici K. Amyotrophic lateral sclerosis--a model of corticofugal axonal spread. *Nat Rev Neurol.* 2013;9(12):708-14.
66. Brettschneider J, Del Tredici K, Toledo JB, Robinson JL, Irwin DJ, Grossman M, Suh E, Van Deerlin VM, Wood EM, Baek Y, et al. Stages of pTDP-43 pathology in amyotrophic lateral sclerosis. *Ann Neurol.* 2013;74(1):20-38.
67. Inayat S, Qandeel, Nazariahangarkolaee M, Singh S, McNaughton BL, Whishaw IQ, and Mohajerani MH. Low acetylcholine during early sleep is important for motor memory consolidation. *Sleep.* 2020;43(6).
68. Gott JA, Stucker S, Kanske P, Haaker J, and Dresler M. Acetylcholine and metacognition during sleep. *Conscious Cogn.* 2024;117(103608.
69. Herrera CG, and Tarokh L. A Thalamocortical Perspective on Sleep Spindle Alterations in Neurodevelopmental Disorders. *Curr Sleep Med Rep.* 2024;10(2):103-18.

70. Brunet A, Stuart-Lopez G, Burg T, Scekic-Zahirovic J, and Rouaux C. Cortical Circuit Dysfunction as a Potential Driver of Amyotrophic Lateral Sclerosis. *Front Neurosci.* 2020;14(363.
71. Luthi A, and Nedergaard M. Anything but small: Microarousals stand at the crossroad between noradrenaline signaling and key sleep functions. *Neuron.* 2025;113(4):509-23.
72. Osorio-Forero A, Cardis R, Vantomme G, Guillaume-Gentil A, Katsioudi G, Devenoges C, Fernandez LMJ, and Luthi A. Noradrenergic circuit control of non-REM sleep substates. *Curr Biol.* 2021;31(22):5009-23 e7.
73. Swift KM, Gross BA, Frazer MA, Bauer DS, Clark KJD, Vazey EM, Aston-Jones G, Li Y, Pickering AE, Sara SJ, et al. Abnormal Locus Coeruleus Sleep Activity Alters Sleep Signatures of Memory Consolidation and Impairs Place Cell Stability and Spatial Memory. *Curr Biol.* 2018;28(22):3599-609 e4.
74. Scekic-Zahirovic J, Benetton C, Brunet A, Ye X, Logunov E, Douchamps V, Megat S, Andry V, Kan VWY, Stuart-Lopez G, et al. Cortical hyperexcitability in mouse models and patients with amyotrophic lateral sclerosis is linked to noradrenaline deficiency. *Sci Transl Med.* 2024;16(738):eadg3665.
75. Bolborea M, Vercruysse P, Daria T, Reiners JC, Alami NO, Guillot SJ, Dieterle S, Sinniger J, Scekic-Zahirovic J, Londo A, et al. Loss of hypothalamic MCH decreases food intake in amyotrophic lateral sclerosis. *Acta Neuropathol.* 2023;145(6):773-91.
76. Vercruysse P, Vieau D, Blum D, Petersen A, and Dupuis L. Hypothalamic Alterations in Neurodegenerative Diseases and Their Relation to Abnormal Energy Metabolism. *Front Mol Neurosci.* 2018;11(16.
77. Gabery S, Ahmed RM, Caga J, Kiernan MC, Halliday GM, and Petersen A. Loss of the metabolism and sleep regulating neuronal populations expressing orexin and oxytocin in the hypothalamus in amyotrophic lateral sclerosis. *Neuropathology and applied neurobiology.* 2021;47(7):979-89.
78. Kolaj M, Zhang L, Hermes ML, and Renaud LP. Intrinsic properties and neuropharmacology of midline paraventricular thalamic nucleus neurons. *Front Behav Neurosci.* 2014;8(132.
79. Govindaiah G, and Cox CL. Modulation of thalamic neuron excitability by orexins. *Neuropharmacology.* 2006;51(3):414-25.
80. Ni KM, Hou XJ, Yang CH, Dong P, Li Y, Zhang Y, Jiang P, Berg DK, Duan S, and Li XM. Selectively driving cholinergic fibers optically in the thalamic reticular nucleus promotes sleep. *eLife.* 2016;5(
81. Lee KH, and McCormick DA. Abolition of spindle oscillations by serotonin and norepinephrine in the ferret lateral geniculate and perigeniculate nuclei in vitro. *Neuron.* 1996;17(2):309-21.
82. Osorio-Forero A, Foustoukos G, Cardis R, Cherrad N, Devenoges C, Fernandez LMJ, and Luthi A. Infraslow noradrenergic locus coeruleus activity fluctuations are gatekeepers of the NREM-REM sleep cycle. *Nat Neurosci.* 2025;28(1):84-96.
83. Brooks BR, Miller RG, Swash M, and Munsat TL. El Escorial revisited: revised criteria for the diagnosis of amyotrophic lateral sclerosis. *Amyotroph Lateral Scler Other Motor Neuron Disord.* 2000;1(5):293-9.
84. Walker NA, Sunderram J, Zhang P, Lu SE, and Scharf MT. Clinical utility of the Epworth sleepiness scale. *Sleep Breath.* 2020;24(4):1759-65.

85. Buysse DJ, Reynolds CF, 3rd, Monk TH, Berman SR, and Kupfer DJ. The Pittsburgh Sleep Quality Index: a new instrument for psychiatric practice and research. *Psychiatry Res.* 1989;28(2):193-213.
86. Ahmed RM, Newcombe RE, Piper AJ, Lewis SJ, Yee BJ, Kiernan MC, and Grunstein RR. Sleep disorders and respiratory function in amyotrophic lateral sclerosis. *Sleep Med Rev.* 2016;26(33-42.
87. Lule D, Burkhardt C, Abdulla S, Bohm S, Kollewe K, Uttner I, Abrahams S, Bak TH, Petri S, Weber M, et al. The Edinburgh Cognitive and Behavioural Amyotrophic Lateral Sclerosis Screen: a cross-sectional comparison of established screening tools in a German-Swiss population. *Amyotrophic lateral sclerosis & frontotemporal degeneration.* 2015;16(1-2):16-23.
88. Abrahams S, Newton J, Niven E, Foley J, and Bak TH. Screening for cognition and behaviour changes in ALS. *Amyotrophic lateral sclerosis & frontotemporal degeneration.* 2014;15(1-2):9-14.
89. Loose M, Burkhardt C, Aho-Ozhan H, Keller J, Abdulla S, Bohm S, Kollewe K, Uttner I, Abrahams S, Petri S, et al. Age and education-matched cut-off scores for the revised German/Swiss-German version of ECAS. *Amyotrophic lateral sclerosis & frontotemporal degeneration.* 2016;17(5-6):374-6.
90. Berry RB, Budhiraja R, Gottlieb DJ, Gozal D, Iber C, Kapur VK, Marcus CL, Mehra R, Parthasarathy S, Quan SF, et al. Rules for scoring respiratory events in sleep: update of the 2007 AASM Manual for the Scoring of Sleep and Associated Events. Deliberations of the Sleep Apnea Definitions Task Force of the American Academy of Sleep Medicine. *J Clin Sleep Med.* 2012;8(5):597-619.
91. Silber MH, Ancoli-Israel S, Bonnet MH, Chokroverty S, Grigg-Damberger MM, Hirshkowitz M, Kapen S, Keenan SA, Kryger MH, Penzel T, et al. The visual scoring of sleep in adults. *J Clin Sleep Med.* 2007;3(2):121-31.
92. Gramfort A, Luessi M, Larson E, Engemann DA, Strohmeier D, Brodbeck C, Goj R, Jas M, Brooks T, Parkkonen L, et al. MEG and EEG data analysis with MNE-Python. *Front Neurosci.* 2013;7(267.
93. Ablin P, Cardoso JF, and Gramfort A. Faster Independent Component Analysis by Preconditioning With Hessian Approximations. *IEEE Transactions on Signal Processing.* 2018;66(15):4040-9.
94. Dammers J, Schiek M, Boers F, Silex C, Zvyagintsev M, Pietrzyk U, and Mathiak K. Integration of amplitude and phase statistics for complete artifact removal in independent components of neuromagnetic recordings. *IEEE Trans Biomed Eng.* 2008;55(10):2353-62.
95. Dharmaprani D, Nguyen HK, Lewis TW, DeLosAngeles D, Willoughby JO, and Pope KJ. A comparison of independent component analysis algorithms and measures to discriminate between EEG and artifact components. *Annu Int Conf IEEE Eng Med Biol Soc.* 2016;2016(825-8.
96. Viola FC, Thorne J, Edmonds B, Schneider T, Eichele T, and Debener S. Semi-automatic identification of independent components representing EEG artifact. *Clin Neurophysiol.* 2009;120(5):868-77.
97. Winkler I, Debener S, Muller KR, and Tangermann M. On the influence of high-pass filtering on ICA-based artifact reduction in EEG-ERP. *Annu Int Conf IEEE Eng Med Biol Soc.* 2015;2015(4101-5.

98. Lacourse K, Delfrate J, Beaudry J, Peppard P, and Warby SC. A sleep spindle detection algorithm that emulates human expert spindle scoring. *J Neurosci Methods.* 2019;316(3-11.
99. Carrier J, Viens I, Poirier G, Robillard R, Lafortune M, Vandewalle G, Martin N, Barakat M, Paquet J, and Filipini D. Sleep slow wave changes during the middle years of life. *Eur J Neurosci.* 2011;33(4):758-66.
100. Virtanen P, Gommers R, Oliphant TE, Haberland M, Reddy T, Cournapeau D, Burovski E, Peterson P, Weckesser W, Bright J, et al. SciPy 1.0: fundamental algorithms for scientific computing in Python. *Nature methods.* 2020;17(3):261-72.
101. Vallat R, and Walker MP. An open-source, high-performance tool for automated sleep staging. *eLife.* 2021;10(
102. Vallat R, and Walker MP. An open-source, high-performance tool for automated sleep staging. *Elife.* 2021;10(e70092.
103. American Academy of Sleep Medicine. Darien, IL, USA: AASM; 2020.
104. Guillot SJ. Sleep spindles detector. Version 2023. https://github.com/sjg2203/SSp_Detector.
105. Guillot SJ. Sl*μ*Arch. Version 2024. https://github.com/sjg2203/SluArch
.
106. Faul F, Erdfelder E, Buchner A, and Lang AG. Statistical power analyses using G*Power 3.1: tests for correlation and regression analyses. *Behav Res Methods.* 2009;41(4):1149-60.
107. Faul F, Erdfelder E, Lang AG, and Buchner A. G*Power 3: a flexible statistical power analysis program for the social, behavioral, and biomedical sciences. *Behav Res Methods.* 2007;39(2):175-91.
108. SHAPIRO SS, and WILK MB. An analysis of variance test for normality (complete samples). *Biometrika.* 1965;52(3-4):591-611.
109. Bartlett MS. Properties of sufficiency and statistical tests. . *Proceedings of the Royal Society of London Series A-Mathematical and Physical Sciences* 1937;160(268-82.
110. Vallat R. Pingouin: statistics in Python. *Journal of Open Source Software.* 2018;3(1026.
111. Zimmerman DW. A note on preliminary tests of equality of variances. *Br J Math Stat Psychol.* 2004;57(Pt 1):173-81.
112. Rouder JN, Speckman PL, Sun D, Morey RD, and Iverson G. Bayesian t tests for accepting and rejecting the null hypothesis. *Psychon Bull Rev.* 2009;16(2):225-37.
113. Seabold S, and Perktold J. *9th Python in Science Conference*. Austin, TX; 2010:25080.
114. Terpilowski M. scikit-posthocs: Pairwise multiple comparison tests in Python. . *Journal of Open Source Software.* 2019;4(1169.
115. Waskom M. seaborn: statistical data visualization. *Journal of Open Source Software* 2021;6(3021.

Figures and legends

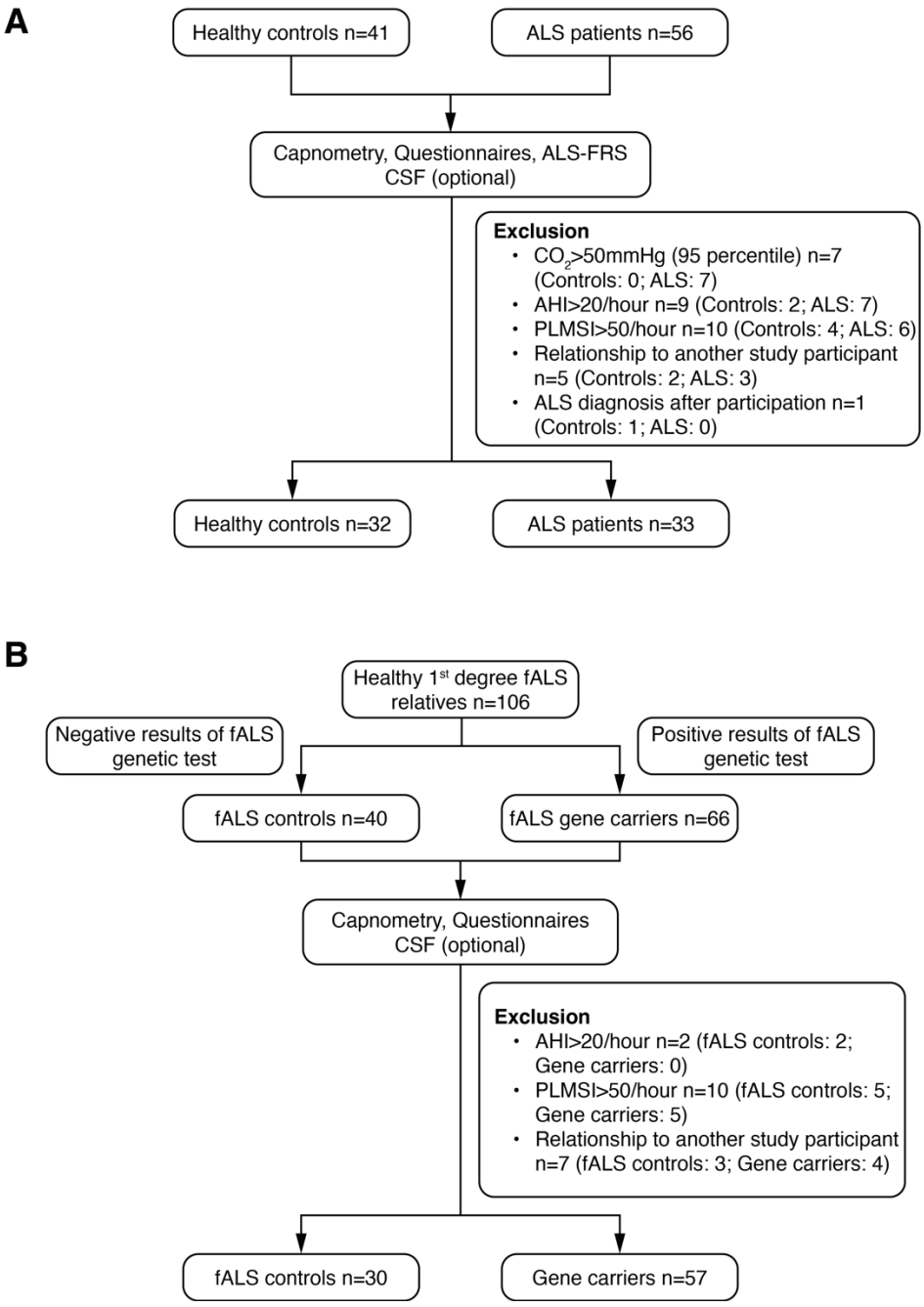

Figure 1: Flowchart of the two cohort studies

Panels A and B show the flowchart of the studies in ALS patients (panel A, same cohort as in (13)) and presymptomatic gene carriers (including additional individuals as in (13)).

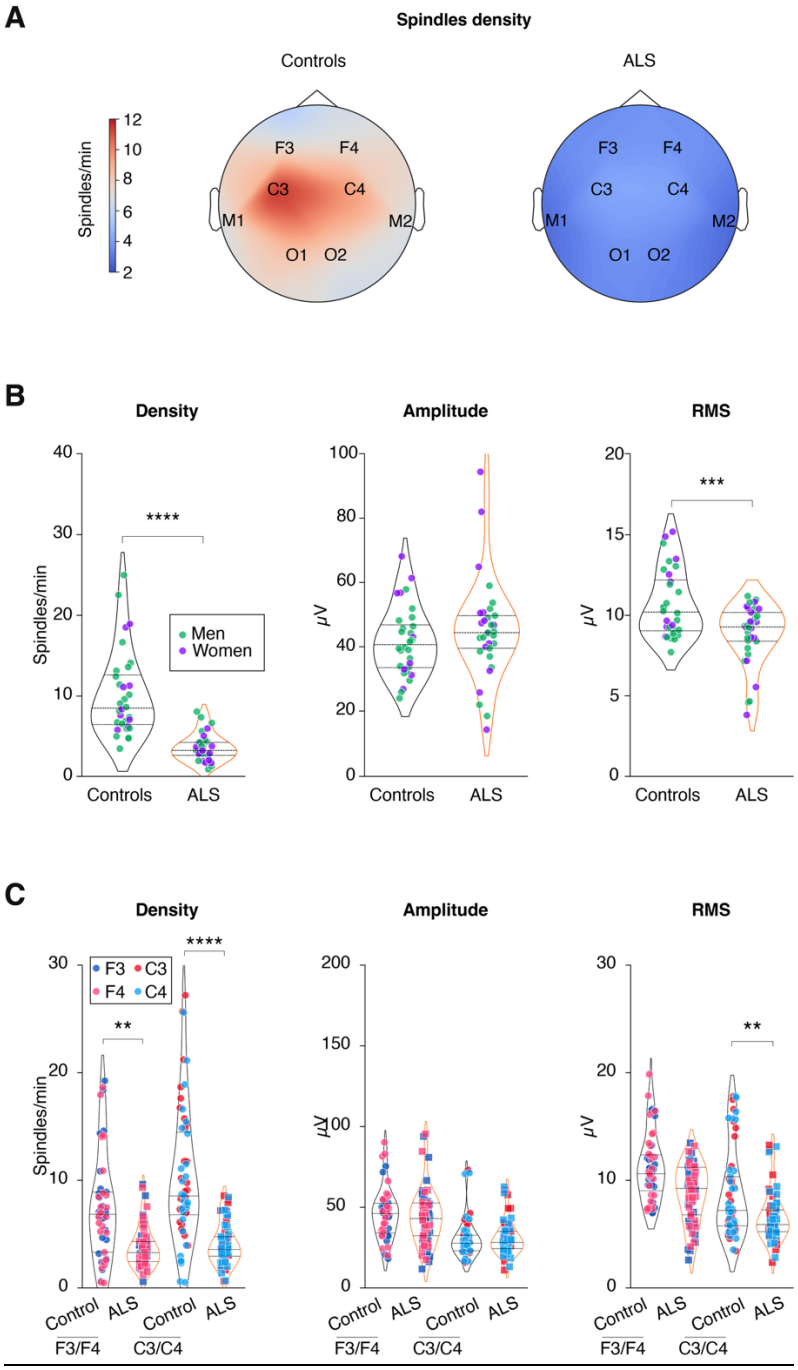

Figure 2: Sleep spindle alterations in early ALS patients.
(**A**) Topographic map across all electrodes of sleep spindle density in controls and ALS patients.
(**B**) Quantification of sleep spindle density, amplitude and root-mean-square (RMS). *** adj. p_{value}<0.001, independent Student's t-test with Welch's t-test correction. Men are shown in green and women in purple.
(**C**) Quantification of sleep spindle density, amplitude and root-mean-square (RMS) across F3/F4 and C3/C4 electrodes as indicated. **** adj. p_{value}<0.0001, ** adj. p_{value}<0.01, Kruskal-Wallis test with Dunn's multiple tests adjusted with FDR-BKY correction.
Results with p_{value}>0.05 are not indicated. Data are presented as medians and interquartile ranges. Corrected p_{value} are shown.

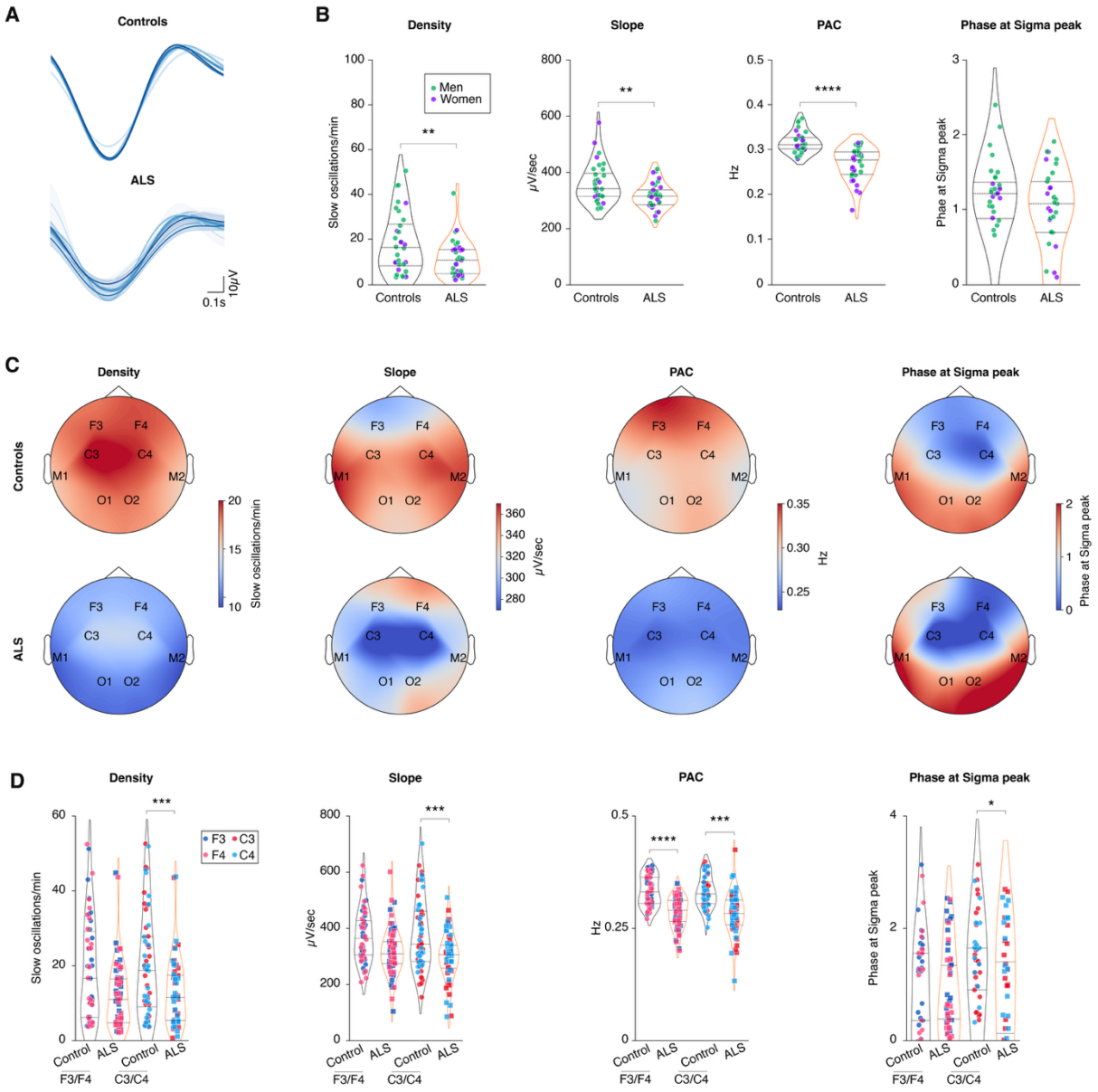

Figure 3: Slow oscillation alterations in early ALS patients.

(**A**) Representative slow oscillations across all electrodes of a healthy individual and one sporadic ALS patient.

(**B**) Quantification of slow oscillation density, slope, phase-amplitude coupling between sleep spindles and slow oscillations (PAC) and phase at Sigma peak (PSP) in controls and ALS patients. ** adj. p_{value}<0.01, **** adj. p_{value}<0.0001, independent Student's t-test with Welch's t-test correction. Men are shown in green and women in purple.

(**C**) Topographic maps across all electrodes of slow oscillation density, slope, phase-amplitude coupling and phase at Sigma peak in Controls (upper row) and ALS patients (lower row).

(**D**) Quantification of slow oscillation density, slope, phase-amplitude coupling and phase at Sigma peak across F3/F4 and C3/C4 electrodes as indicated. * adj. p_{value}<0.05, *** adj. p_{value}<0.001, **** adj. p_{value}<0.0001, Kruskal-Wallis test with Dunn's multiple tests adjusted with FDR-BKY correction.

Results with p_{value}>0.05 are not indicated. Data are presented as medians and interquartile ranges. Corrected p_{value} are shown.

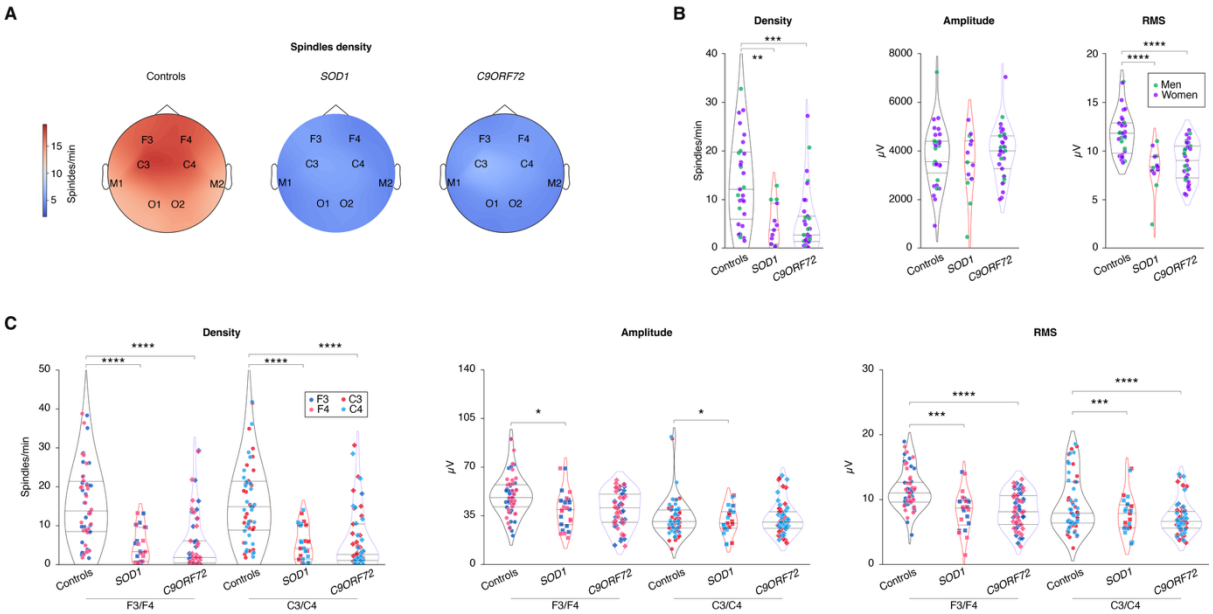

Figure 4: Sleep spindle alterations in presymptomatic ALS gene carriers.

(**A**) Topographic map across all electrodes of sleep spindle density in controls, *SOD1* and *C9ORF72* presymptomatic gene carriers.

(**B**) Quantification of sleep spindle density, amplitude and root-mean-square (RMS) in controls, *SOD1* and *C9ORF72* presymptomatic gene carriers. *** adj. p_{value}<0.001, **** adj. p_{value}<0.0001, One-way ANOVA with FDR-BKY correction. Men are shown in green and women in purple.

(**C**) Quantification of sleep spindle density, amplitude and root-mean-square (RMS) in controls, *SOD1* and *C9ORF72* presymptomatic gene carriers across F3/F4 and C3/C4 electrodes as indicated. * adj. p_{value}<0.05, *** adj. p_{value}<0.001, **** adj. p_{value}<0.0001, Kruskal-Wallis test with Dunn's multiple tests adjusted with FDR-BKY correction.

Results with p_{value}>0.05 are not indicated. Data are presented as medians and interquartile ranges. Corrected p_{value} are shown.

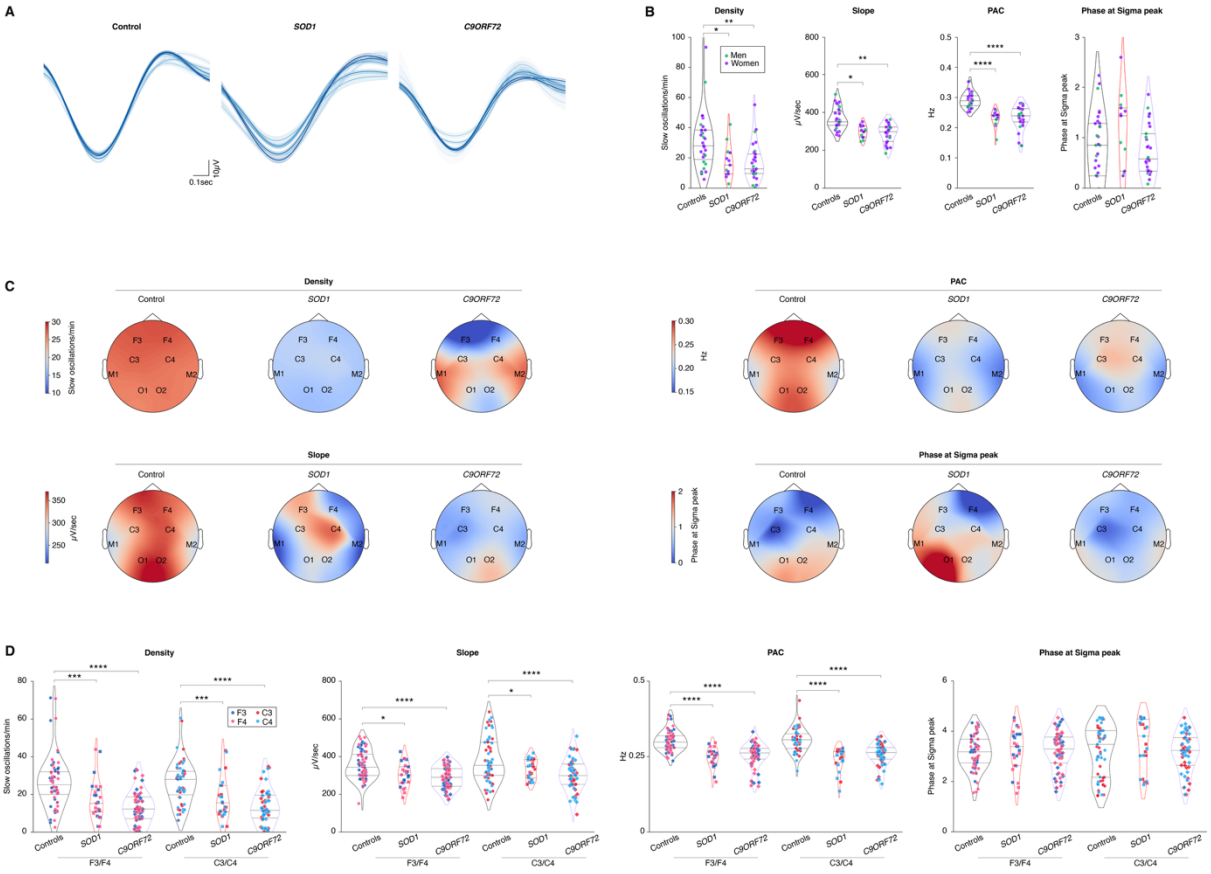

Figure 5: Slow oscillation alterations in presymptomatic ALS gene carriers.

(**A**) Representative slow oscillations across all electrodes of a healthy individual and one presymptomatic *SOD1* and *C9ORF72* gene carrier.

(**B**) Quantification of slow oscillation density, slope, phase-amplitude coupling between sleep spindles and slow oscillations (PAC) and phase at Sigma peak (PSP) in controls, *SOD1* and *C9ORF72* presymptomatic gene carriers. * adj. p_{value}<0.05, ** adj. p_{value}<0.01, **** adj. p_{value}<0.0001, One-way ANOVA with FDR-BKY correction. Men are shown in green and women in purple.

(**C**) Topographic maps across all electrodes of slow oscillation density, slope, phase-amplitude coupling and phase at Sigma peak in controls, *SOD1* and *C9ORF72* presymptomatic gene carriers.

(**D**) Quantification of slow oscillation density, slope, phase-amplitude coupling and phase at Sigma peak across F3/F4 and C3/C4 electrodes in controls, *SOD1* and *C9ORF72* presymptomatic gene carriers as indicated. * adj. p_{value}<0.05, *** adj. p_{value}<0.001, **** adj. p_{value}<0.0001, Kruskal-Wallis test with Dunn's multiple tests adjusted with FDR-BKY correction.

Results with p_{value}>0.05 are not indicated. Data are presented as medians and interquartile ranges. Corrected p_{value} are shown.

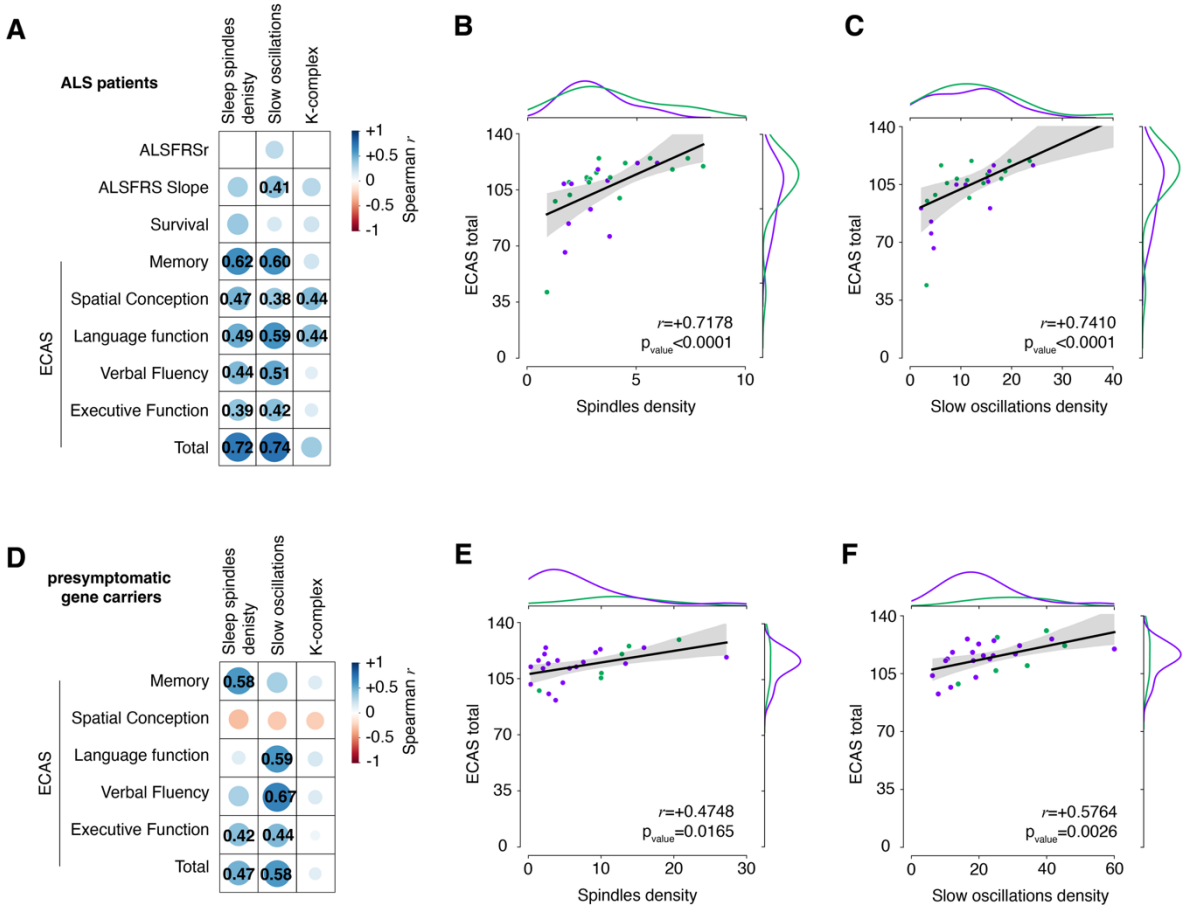

Figure 6: Correlation analysis between sleep microarchitecture, cognitive function and motor function in ALS patients and presymptomatic gene carriers.

(**A**) Correlation matrix showing Spearman correlation coefficient *r* for each of the corresponding correlations performed in ALS patients. Sleep spindle density, slow oscillation density and K-complex density were correlated with ALSFRSr, ALSFRS slope, patients' survival and ECAS subscores as well as the total score for all ALS patients. Only significant correlations are indicated, with the numerical value of the Spearman *r.*

(**B-C)** Correlation between total ECAS scores and sleep spindle density (B) or slow oscillations density (C) in ALS patients.

(**D**) Correlation matrix showing Spearman correlation coefficient *r* for each of the corresponding correlations performed in presymptomatic gene carriers. Sleep spindle density, slow oscillation density and K-complex density were correlated with ECAS subscores as well as the total score for all *SOD1* and *C9ORF72* gene carriers. Only significant correlations are indicated, with the numerical value of the Spearman *r.*

(**E-F)** Correlation between total ECAS scores and sleep spindle density (B) or slow oscillations density (C) in presymptomatic gene carriers.

In all panels, men are shown in green and women in purple.

Spearman pvalue was adjusted with FDR-BKY correction. Spearman correlation coefficient *r* and corrected pvalue are indicated. Side distribution represents sex distribution across both variables (men in green, women in purple).

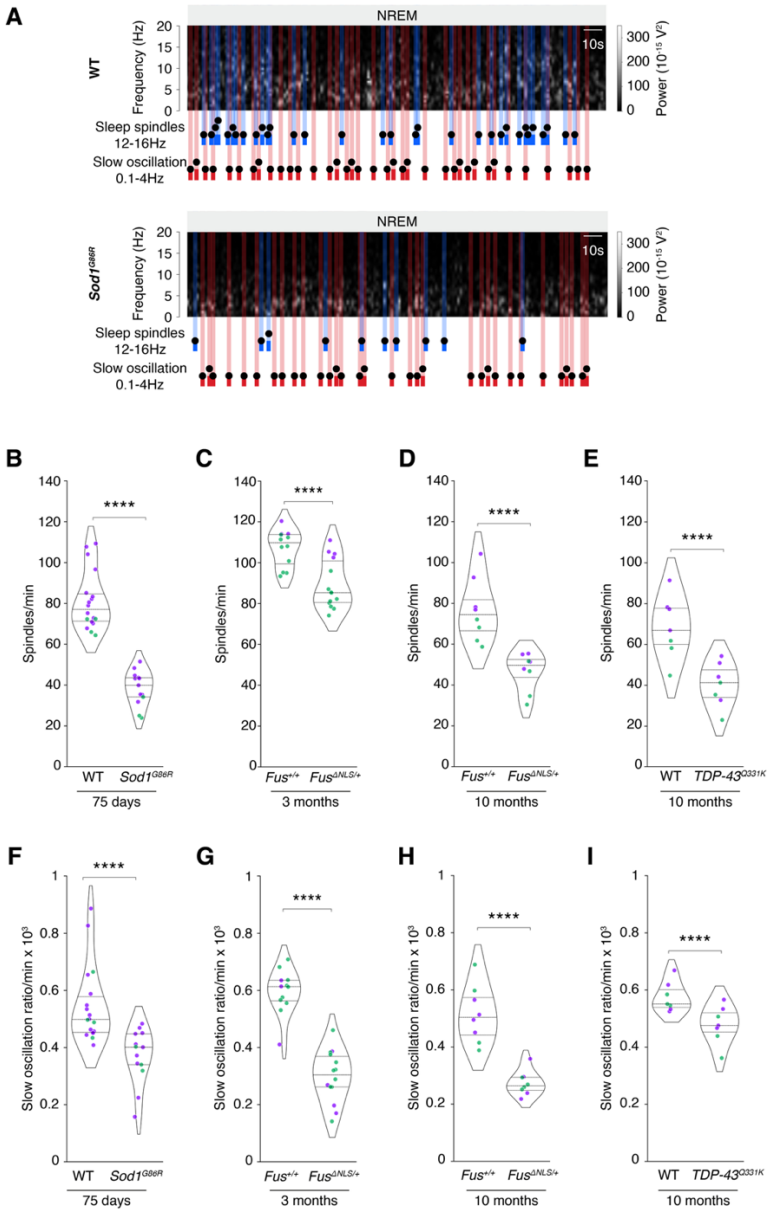

Figure 7: Sleep microarchitecture alterations in *Sod1*^{G86R}, *Fus*$^{\Delta NLS/+}$ and *TDP-43*^{Q331K} mice.

(**A**) Representative spectrogram of *Sod1*^{G86R} mice and their non-transgenic wild-type (WT) littermates at 75 days of age (prior to motor symptom onset). Sleep spindles are labelled in blue and slow oscillation in red on the spectrogram.

(**B-I**) Quantification of sleep spindle density (B-E) and slow oscillation density (F-I) in *Sod1*^{G86R} mice and their non-transgenic WT littermates at 75 days of age (B, F), in *Fus*$^{\Delta NLS/+}$ mice and their WT littermates (*Fus*$^{+/+}$) at 3 months of age (C, G, prior to motor symptom onset) or at 10 months of age (D, H) and in TDP-43^{Q331K} mice at 10 months of age (E, I).

Independent Student's t-test with Welch's t-test with FRD-BKY correction; Data are presented as medians and interquartile ranges. Corrected p_{value} are shown. **** adj. p_{value}<0.0001,

Sleep spindle density: Sex effect *Sod1*^{G86R} adj. p_{value}=0.0238, *Fus*$^{\Delta NLS/+}$ 3 months adj. p_{value}=0.0183, *Fus*$^{\Delta NLS/+}$ 10 months adj. p_{value}=0.0455, *TDP-43*^{Q331K} 10 months adj. p_{value}=0.0863.

Slow oscillations density: Sex effect *Sod1*^{G86R} adj. p_{value}=0.7128, *Fus*$^{\Delta NLS/+}$ 3 months adj. p_{value}=0.2740, *Fus*$^{\Delta NLS/+}$ 10 months adj. p_{value}=0.8112, *TDP-43*^{Q331K} 10 months adj. p_{value}=0.3648.

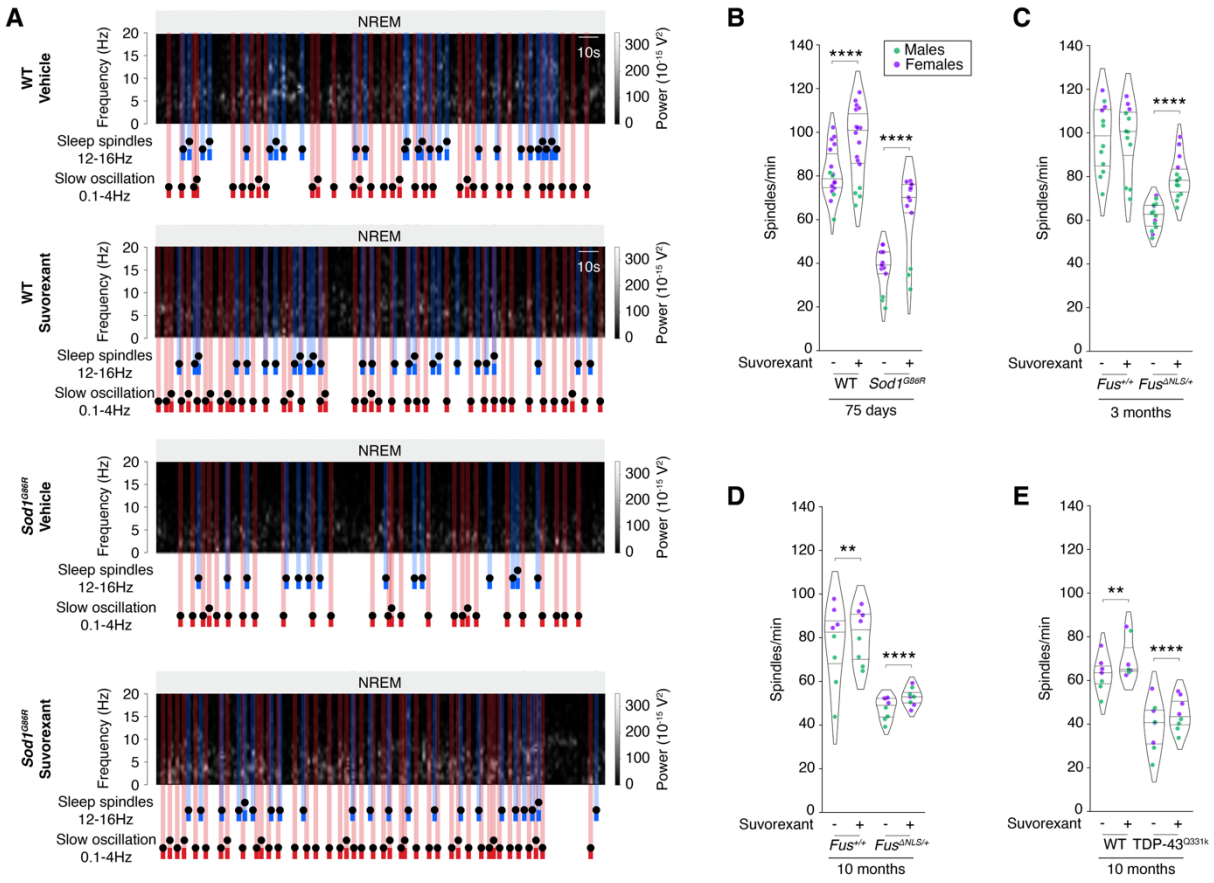

Figure 8: Improved sleep microarchitecture by Suvorexant *Sod1^{G86R}*, *Fus$^{ΔNLS/+}$* and *TDP-43^{Q331K}* mice.

(**A**) Representative spectrogram of *Sod1^{G86R}* mice and their non-transgenic wild-type (WT) littermates at 75 days of age (prior to motor symptom onset) administered with either vehicle or Suvorexant. Sleep spindles are labelled in blue and slow oscillation in red on the spectrogram.

(**B-E**) Quantification of sleep spindle density in mice treated with either vehicle or suvorexant. Genotypes studied include *Sod1^{G86R}* mice and their non-transgenic WT littermates at 75 days of age (B), in *Fus$^{ΔNLS/+}$* mice and their WT littermates (*Fus$^{+/+}$*) at 3 months of age (C, prior to motor symptom onset) or at 10 months of age (D) and in TDP-43^{Q331K} mice at 10 months of age (E)

ns adj. p_{value}>0.05, Two-Way ANOVA with Dunn's test and FDR-BKY correction. Genotype effect *Sod1*^{G86R} adj. p_{value}<0.0001, *Fus$^{ΔNLS/+}$* 3 months adj. p_{value}<0.0001, *Fus$^{ΔNLS/+}$* 10 months adj. p_{value}<0.0001, *TDP-43*^{Q331K} 10 months adj. p_{value}<0.0001; sex effect *Sod1*^{G86R} adj. p_{value}<0.0001, *Fus$^{ΔNLS/+}$* 3 months adj. p_{value}=0.4584, *Fus$^{ΔNLS/+}$* 10 months adj. p_{value}=0.3032, *TDP-43*^{Q331K} 10 months adj. p_{value}=0.1522. Data are presented as medians and interquartile ranges. Corrected p_{value} are shown.

Tables

Table 1: Descriptive statistics of the study population of ALS patients and healthy controls.
SEM: standard error of means; BMI: body mass index; ALSFRSr: Amyotrophic Lateral Sclerosis Functional Rating Scale-Revised. Non-parametric Kruskal-Wallis' test, ns $p_{value}>0.05$.

		ALS	Controls	p_{value}	Reference
Gender	Women (%)	14 (42.4)	10 (31.3)		
	Men (%)	19 (57.6)	22 (68.7)		
BMI mean (±SEM)		26.38 (±0.78)	26.63 (±0.77)	0.885	(13)
Age mean (±SEM)		58.56 (±1.74)	56.22 (±2.81)	0.652	
ALSFRSr mean (±SEM)		40.51 (0.78)	—		

Table 2: Descriptive statistics of the study population of fALS participants.
SEM: standard error of means; BMI: body mass index. Non-parametric Kruskal-Wallis' test, ns $p_{value}>0.05$.

		Gene Carriers	Controls	p_{value}
Population 1 - previously described in (13)				
Gender	Women (%)	20 (71.4)	14 (73.7)	
	Men (%)	8 (28.6)	5 (26.3)	
BMI mean (±SEM)		26.88 (±0.89)	26.06 (±1.59)	0.72
Age mean (±SEM)		40.66 (±2.88)	41.84 (±2.67)	0.81
Population 2 - This study				
Gender	Women (%)	20 (69)	7 (63.6)	
	Men (%)	9 (31)	4 (36.4)	
BMI mean (±SEM)		25.62 (±1.30)	26.94 (±2.172)	0.629
Age mean (±SEM)		40.71 (±3.04)	43 (±4.37)	0.71